

# Sommerfeld enhancements with vector, scalar and pseudoscalar force-carriers

Ze-Peng Liu<sup>a\*</sup>, Yue-Liang Wu<sup>a,b†</sup>, and Yu-Feng Zhou<sup>a‡</sup>

*<sup>a</sup>State Key Laboratory of Theoretical Physics,  
Kavli Institute for Theoretical Physics China,  
Institute of Theoretical Physics, Chinese Academy of Sciences  
Beijing, 100190, P.R. China*

*<sup>b</sup>University of Chinese Academy of Sciences,  
Beijing, 100049, P.R. China*

## Abstract

The first AMS-02 measurement confirms the existence of an excess in the cosmic-ray positron fraction previously reported by the PAMELA and Fermi-LAT experiments. If interpreted in terms of thermal dark matter (DM) annihilation, the AMS-02 result still suggests that the DM annihilation cross section in the present day should be significantly larger than that at freeze out. The Sommerfeld enhancement of DM annihilation cross section is a possible explanation, which is however subject to the constraints from DM thermal relic density, mainly due to the annihilation of DM particles into force-carrier particles introduced by the mechanism. We show that the effects of the Sommerfeld enhancement and the relic density constraints depend significantly on the nature of the force-carrier. Three scenarios where the force-carrier is a vector boson, scalar and pseudoscalar particle are investigated and compared. The results show that for the case with vector force-carrier, the Sommerfeld enhancement can marginally account for the AMS-02 data for DM particle annihilating into  $2\mu$  final states, while for scalar force-carrier the allowed Sommerfeld enhancement factor can be larger by a factor of two. For the case with a pseudoscalar force-carrier, the Sommerfeld enhancement factor can be very large in the resonance region, and it is possible to accommodate the AMS-02 and Fermi-LAT result for a variety of DM annihilation final states.

---

\*Email: zpliu@itp.ac.c

†Email: ylwu@itp.ac.cn

‡Email: yfzhou@itp.ac.cn

# 1 Introduction

Evidence from astronomical observations at different scales has indicated that dark matter (DM) contributes to nearly 26% of the energy density of the Universe [1, 2]. Popular DM candidates such as the weakly interacting massive particles (WIMPs) are expected to annihilate or decay into standard model (SM) final states in the Galactic halo and beyond, which may leave imprints in the fluxes of cosmic-ray particles.

In the recent years, the PAMELA collaboration has reported a sharp upturn of the ratio of the positron flux to the total flux of electrons and positrons in the energy range  $\sim 10 - 100$  GeV, which is in excess over a conventional astrophysical background [3, 4], and was confirmed by the Fermi-LAT data up to  $\sim 200$  GeV [5]. The total fluxes of electrons and positrons measured by ATIC [6] and Fermi-LAT [7, 8] also showed possible excesses over the expectations of the conventional background. Recently, the AMS-02 collaboration released the first measurement of the positron fraction with unprecedented accuracy [9]. Although the AMS-02 data are consistent with the previous measurements of PAMELA, the measured spectrum from AMS-02 is slightly lower than that from PAMELA for electron/positron energy higher than  $\sim 40$  GeV, and the slope of the positron fraction decreases by an order of magnitude from  $\sim 20$  GeV to  $\sim 250$  GeV. The implications of the precision AMS-02 data on the DM annihilation have been discussed (see e.g. Refs. [10–17]). Several fits to the AMS-02 data showed that if  $2\mu$  is the dominant DM annihilation channel, the AMS-02 favoured DM particle mass is  $\sim 400 - 500$  GeV, and the thermally averaged product of annihilation cross section and relative velocity is  $\langle\sigma v_{\text{rel}}\rangle \sim 10^{-24} \text{ cm}^3 \text{ s}^{-1}$  [11, 14, 17]. For instance, in Ref. [14], using a conventional astrophysical background, the best fitted DM particle mass is found to be  $m_\chi \approx 460$  GeV, with an annihilation cross section  $\langle\sigma v_{\text{rel}}\rangle \approx 1.9 \times 10^{-24} \text{ cm}^3 \text{ s}^{-1}$ . The DM annihilating into  $2e$  is not favoured as the predicted positron spectrum is too hard. For  $2\tau$  final states, the favoured DM particle mass is  $\sim 1.4$  TeV and the annihilation cross section  $\sim 1.7 \times 10^{-23} \text{ cm}^3 \text{ s}^{-1}$ , which is compatible with the Fermi-LAT data [14]. Note that the  $2\tau$  final states can generate large flux of diffuse gamma rays which is stringently constrained by the current observations. Although it seems that the favoured parameter regions by the current AMS-02 data are different from that by Fermi-LAT for some leptonic final states, all the current experimental data suggest that the DM annihilation cross section in the present day must be larger than the typical WIMP thermal cross section  $\langle\sigma v_{\text{rel}}\rangle_F \approx 3 \times 10^{-26} \text{ cm}^3 \text{ s}^{-1}$  at freeze out, which calls for nonstandard nature of DM particles.

The Sommerfeld enhancement has been considered as a mechanism which can naturally enhance the DM annihilation cross section at low relative velocities [18–26]. (for other mechanisms, see e.g. [27–31]). In this scenario, the cross section of the DM anni-

hilation  $\bar{\chi}\chi \rightarrow X$  ( $X = 2\mu, 4\mu, \dots$ ) is velocity-dependent, due to the multiple exchange of some light force-carrier particle  $\phi$  between the annihilating DM particles  $\bar{\chi}\chi$ . The thermally averaged annihilation cross section can be close to  $\langle\sigma v_{\text{rel}}\rangle_F$  at the time of thermal freeze out, but becomes much larger now as the temperature of the Universe in the present day is much lower. Constraints on the Sommerfeld enhancement can be obtained from astrophysical observations (see e.g. Refs. [32–43]). Among them, a stringent constraint on the Sommerfeld enhancement can arise from the DM thermal relic density itself, which is less sensitive to the astrophysical uncertainties. This is due to the fact that, in this mechanism, the DM particles inevitably annihilate into the force-carriers through the process like  $\bar{\chi}\chi \rightarrow \phi\phi$ , which enhances the DM total annihilation cross section at freeze out, and the relevant parameters are constrained by the DM relic density. This reduces the allowed values of the Sommerfeld enhancement factor at lower temperature [38, 44]. Based on a model in which  $\phi$  is a  $U(1)$  vector gauge boson, it has been illustrated that under the relic density constraint, the Sommerfeld enhancement factor is not large enough to account for the excesses reported by the PAMELA and Fermi-LAT experiments [38, 44]. Note that the Sommerfeld enhancement can be realized with different type of force-carriers, such as scalar and pseudoscalar particles [22, 45, 46]. An  $U(1)$  vector gauge bosons can be naturally light under the protection of gauge symmetry. A pseudoscalar particles can also be naturally light if they play the role of a pseudo-Goldstone boson. A light scalar particle can be stable with the help of supersymmetry. The effect of the Sommerfeld enhancement and the constraint from thermal relic density depend on the nature of the force-carrier particle. For instance, if  $\phi$  is a scalar particle, the cross section for  $\bar{\chi}\chi \rightarrow \phi\phi$  is velocity suppressed, resulting in a weaker constraint compared with the case where  $\phi$  is a vector boson. If  $\phi$  is a pseudoscalar, the induced potential is of tensor force type rather than the Yukawa type.

In light of the recent AMS-02 results, it is of interest to investigate whether the Sommerfeld enhancement can account for the more accurate AMS-02 data in generic cases. In this work, we explore and compare the Sommerfeld enhancements with three different type of force-carriers: vector, scalar and pseudoscalar, under the constraint from DM thermal relic density. We show that for vector boson force-carrier the Sommerfeld enhancement can only marginally account for the AMS-02 data, for scalar force-carrier the allowed Sommerfeld enhancement factor can be larger roughly by a factor of two, while in the case of pseudoscalar force carrier, much larger enhancement can be obtained in the resonance region.

This paper is organized as follows. In Sec. 2, we outline the formalism of the Sommerfeld enhancement and the thermal evolution of the DM number density. In Sec. 3, we discuss the Sommerfeld enhancement and the constraints for the cases with vector, scalar

and pseudoscalar force carriers, and compare the allowed enhancement factors with the current experimental data. The nature of Sommerfeld enhancement with pseudoscalar is discussed in detail. The conclusions are given in Sec. 4.

## 2 Mechanism of Sommerfeld enhancement

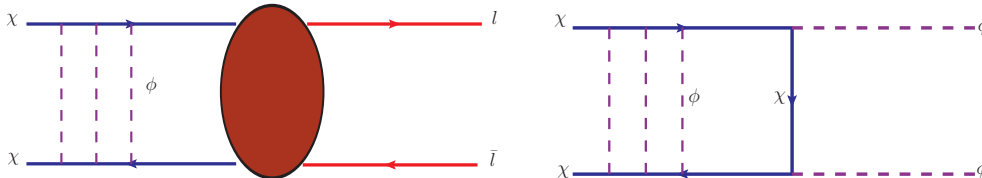


FIG. 1: (Left) Feynman diagram of DM annihilation process  $\bar{\chi}\chi \rightarrow X$ , ( $X = 2\mu, 2\tau, \dots$ ) with multiple force-carrier exchange which results in Sommerfeld enhancement of the annihilation cross section. (Right) Feynman diagram of DM annihilation into the force-carriers through  $t$ -channel process  $\bar{\chi}\chi \rightarrow 2\phi$ .

The Sommerfeld enhancement of DM particle annihilation cross section occurs when the annihilating particles self-interact through a long-range attractive potential  $V(\mathbf{r})$  at low relative velocities [18]. In this scenario, the short-distance DM particle annihilation cross section can be greatly enhanced due to the distortion of the wave function of the annihilating particles at the origin [19–21, 47]. The attractive potential can be induced from the multiple-exchange of some light force-carrier particle  $\phi$  between the annihilating DM particles as shown in the left panel of Fig. 1. The nature of Sommerfeld enhancement has been extensively studied (see e.g. Refs. [22, 25, 26, 32, 38, 44, 48–54]) in light of the cosmic-ray positron/electron excesses reported by PAMELA [3], ATIC [6], and Fermi-LAT [7] etc..

The effect of Sommerfeld enhancement can be described by the following non-relativistic Schrödinger equation for the two-body wave function  $\Psi(\mathbf{r})$  of the annihilating DM particles

$$-\frac{1}{m_\chi}\nabla^2\Psi(\mathbf{r}) + V(\mathbf{r})\Psi(\mathbf{r}) = \frac{m_\chi v_{\text{rel}}^2}{4}\Psi(\mathbf{r}), \quad (1)$$

where  $\mathbf{r}$  and  $v_{\text{rel}}$  are the relative distance and velocity of the two annihilating DM particles, respectively. After an expansion over the Legendre polynomial  $P_\ell(\cos\theta)$  with angular momentum  $\ell$ , namely,  $\Psi(r, \theta) = \sum_\ell P_\ell(\cos\theta)\chi_\ell(r)/r$ , with  $r = |\mathbf{r}|$  and  $\theta$  the zenith angle of spherical coordinates, the Schrödinger equation for radial wave function

$\chi_\ell(r)$  can be written as

$$\frac{d^2\chi_\ell(r)}{dr^2} - \sum_{\ell'} \left[ m_\chi V_{\ell\ell'}(r) + \frac{\ell(\ell+1)}{r^2} \delta_{\ell\ell'} \right] \chi_{\ell'}(r) + k^2 \chi_\ell(r) = 0, \quad (2)$$

where  $k \equiv m_\chi v_{\text{rel}}/2$  and  $V_{\ell\ell'}$  is given by

$$V_{\ell\ell'}(r) = \frac{(2\ell+1)}{2} \int_{-1}^{+1} P_\ell(\cos\theta) V(r, \theta) P_{\ell'}(\cos\theta) d(\cos\theta). \quad (3)$$

The above Schrödinger equation can be solved with the following boundary conditions [25, 26]

$$\lim_{r \rightarrow 0} \chi_\ell(r) = (kr)^{\ell+1} \quad \text{and} \quad \lim_{r \rightarrow 0} \frac{d\chi_\ell(r)}{dr} = k(\ell+1)(kr)^\ell. \quad (4)$$

The asymptotic behaviour of the wave function at infinity is

$$\lim_{r \rightarrow \infty} \chi_\ell(r) \rightarrow C_\ell \sin\left(kr - \frac{\pi}{2}\ell + \delta_\ell\right), \quad (5)$$

where  $\delta_\ell$  is the phase shift and  $C_\ell$  is a normalization constant. With the aforementioned boundary conditions, the Sommerfeld enhancement factor  $S_\ell$  for a partial wave  $\ell$  is given by [22, 25]

$$S_\ell \equiv \lim_{r \rightarrow 0} \left| \frac{\chi_\ell(r)}{\chi_\ell^{(0)}(r)} \right|^2 = \left[ \frac{(2\ell+1)!!}{C_\ell} \right]^2, \quad (6)$$

where  $\chi_\ell^{(0)}(r)$  is the wave function in the free-motion case without a potential.

The exchange of a massive vector or scalar particle  $\phi$  with mass  $m_\phi$  between the DM particles results in an attractive Yukawa potential

$$V(r) = -\frac{\alpha e^{-m_\phi r}}{r}, \quad (7)$$

where  $\alpha$  is the coupling strength. In the limit of  $4\alpha m_\phi/m_\chi \ll v_{\text{rel}}^2$ , the Yukawa potential in the Schrödinger equation can be well approximated by a Coulomb-type potential, and the Schrödinger equation can be solved analytically for arbitrary angular momentum. The enhancement factors read [26]

$$S_0(v_{\text{rel}}) \approx \left( \frac{2\pi\alpha}{v_{\text{rel}}} \right) \frac{1}{1 - e^{-2\pi\alpha/v_{\text{rel}}}}, \quad \text{and} \quad S_1(v_{\text{rel}}) \approx S_0(v_{\text{rel}}) \left( 1 + \frac{\pi^2\alpha^2}{v_{\text{rel}}^2} \right). \quad (8)$$

Therefore, at low velocities, the  $s$ - and  $p$ -wave Sommerfeld enhancement factors scale as  $v_{\text{rel}}^{-1}$  and  $v_{\text{rel}}^{-3}$  respectively. In the case where  $m_\phi$  is non-negligible, the  $v_{\text{rel}}^{-1}$  behavior of  $s$ -wave cross section breaks down. Through approximating the Yukawa potential by

the Hulthén potential, the  $s$ -wave Sommerfeld enhancement factor can be estimated as [26, 49]

$$S_0(v_{\text{rel}}) \approx \left( \frac{2\pi\alpha}{v_{\text{rel}}} \right) \frac{\sinh\left(\frac{6v_{\text{rel}}m_\chi}{\pi m_\phi}\right)}{\cosh\left(\frac{6v_{\text{rel}}m_\chi}{\pi m_\phi}\right) - \cos\left(\sqrt{\frac{24\alpha m_\chi}{m_\phi} - \frac{36m_\chi^2 v_{\text{rel}}^2}{\pi^2 m_\phi^2}}\right)}. \quad (9)$$

For  $4\alpha m_\phi \gg v_{\text{rel}}^2$ , namely, the deBroglie wavelength of incoming particles is much longer than the range of the interaction, the  $s$ -wave Sommerfeld enhancement saturates with  $S_0 \sim 12/\epsilon_\phi$  where  $\epsilon_\phi \equiv m_\phi/(\alpha m_\chi)$ . But for some particular values of  $\epsilon_\phi \simeq 6/(\pi^2 n^2)$ , ( $n = 1, 2, 3, \dots$ ) at which the DM particle can form zero-energy bound states, there exists additional resonant enhancements which scale as  $v_{\text{rel}}^{-2}$ . The resonant enhancement is eventually cut off by the finite width of the resonance [22].

The velocity dependence of  $p$ -wave enhancement was investigated in Refs. [25, 26, 48, 55]. Its effect on the freeze out and thermal relic density was studied in detail in Ref. [56]. The generic  $p$ -wave annihilation cross section before including the Sommerfeld enhancement is proportional to  $v_{\text{rel}}^2$ . Thus the velocity dependence of the total Sommerfeld-enhanced  $p$ -wave annihilation cross section should be proportional to  $S_1 v_{\text{rel}}^2$ . As shown in Ref. [56], in the region where  $\epsilon_\phi \lesssim 10^{-3}$ , the total annihilation cross section scales as  $v_{\text{rel}}^{-1}$  instead of  $v_{\text{rel}}^{-3}$ . In the resonance region  $10^{-3} \lesssim \epsilon_\phi \lesssim 10^{-1}$ , the velocity dependence of  $S_1 v_{\text{rel}}^2$  is not significant. In the saturation region  $\epsilon_\phi \gtrsim 10^{-1}$ ,  $S_1 v_{\text{rel}}^2$  scales as  $v_{\text{rel}}^2$ , the total cross section decreases rapidly towards low velocities. Thus the main difference from the  $s$ -wave case is that the total  $p$ -wave annihilation cross section can be either velocity-suppressed or velocity-enhanced, depending on the values of  $\epsilon_\phi$ .

The generic DM annihilation cross section times the relative velocity before including the Sommerfeld enhancement has the form  $(\sigma v_{\text{rel}})_0 = a + b v_{\text{rel}}^2 + \mathcal{O}(v_{\text{rel}}^4)$ , where  $a$  and  $b$  are coefficients corresponding to the  $s$ - and  $p$ -wave contributions which are assumed to be velocity-independent. After including the Sommerfeld enhancement, the thermally averaged cross section at a temperature  $T$  or  $x \equiv m_\chi/T$  can be written as

$$\langle \sigma v_{\text{rel}} \rangle(x) = a \langle S_0(v_{\text{rel}}) \rangle(x) + b \langle S_1(v_{\text{rel}}) v_{\text{rel}}^2 \rangle(x), \quad (10)$$

where the thermal average of a quantity  $\mathcal{X}(v_{\text{rel}})$  in the non-relativistic limit is given by

$$\langle \mathcal{X} \rangle(x) = \frac{x^{3/2}}{2\sqrt{\pi}} \int_0^\infty \mathcal{X}(v_{\text{rel}}) e^{-\frac{x v_{\text{rel}}^2}{4}} v_{\text{rel}}^2 dv_{\text{rel}}. \quad (11)$$

Due to the Sommerfeld enhancement, the thermally averaged annihilation cross section  $\langle \sigma v_{\text{rel}} \rangle(x)$  depends on the parameters  $\alpha$  and  $m_\phi$ .

The temporal evolution of the DM number density is governed by the Boltzmann equation

$$\frac{dY}{dx} = -\sqrt{\frac{\pi}{45}} m_{\text{Pl}} m_\chi \frac{g_{*s} g_*^{-1/2}}{x^2} \langle \sigma v_{\text{rel}} \rangle [Y^2 - (Y^{\text{eq}})^2], \quad (12)$$

where  $Y^{(\text{eq})} \equiv n_\chi^{(\text{eq})}/s$  is the (equilibrium) number density rescaled by entropy density  $s$ ,  $m_{\text{Pl}} \simeq 1.22 \times 10^{19}$  GeV is the Planck mass scale.  $g_{*s}$  and  $g_*$  are the effective relativistic degrees of freedom for entropy and energy density, respectively.

The DM number density in the present day can be obtained by integrating Eq. (12) with respect to  $x$  in the region  $x_f \leq x \leq x_{\text{now}}$ , where  $x_f \approx 25$  is the decoupling temperature, and  $x_{\text{now}} \approx 4 \times 10^6$  corresponds to the temperature of halo DM in the present day

$$\frac{1}{Y(x_{\text{now}})} = \frac{1}{Y(x_f)} + \sqrt{\frac{\pi}{45}} m_{\text{Pl}} m_\chi \int_{x_f}^{x_s} \frac{g_{*s} g_*^{-1/2}}{x^2} \langle \sigma v_{\text{rel}} \rangle dx. \quad (13)$$

Finally, the relic abundance of DM particles is given by  $\Omega h^2 \approx 2.76 \times 10^8 Y(x_{\text{now}}) (m_\chi/\text{GeV})$ , which is to be compared with the observed value [2]

$$(\Omega h^2)_{\text{exp}} = 0.1187 \pm 0.0017. \quad (14)$$

In this work, we solve the Eq. (12) directly using numerical approaches.

### 3 Sommerfeld enhancement and relic density constraints with different force-carriers

The presence of Sommerfeld enhancement modifies the calculation of the DM thermal relic density. First, the Sommerfeld-enhanced cross section of  $\bar{\chi}\chi \rightarrow X$  increases with  $x$  during freeze out, which postpones the decoupling of DM particles from the thermal bath and results in a decrease of the DM relic density [32, 51]. Second, as the force-carrier is much lighter than the DM particle, i.e.,  $m_\phi \ll m_\chi$ , the DM particles necessarily annihilate into the force-carriers. The process like  $\bar{\chi}\chi \rightarrow \phi\phi$  will contribute to an annihilation channel in addition to  $\bar{\chi}\chi \rightarrow X$ , and can even be the dominant contribution to the total DM annihilation cross section, which further reduces the DM relic density. Thus in order to reproduce the observed DM relic density, the relevant parameters such as the coupling  $\alpha$  has to be small enough, which results in a reduction of the Sommerfeld enhancement factors at low temperatures [38, 44]. Before switching on the effect of Sommerfeld enhancement, the total DM annihilation cross section  $(\sigma_{\text{tot}} v_{\text{rel}})_0$  can be written as the sum of the two contributions, namely,  $(\sigma_{\text{tot}} v_{\text{rel}})_0 = (\sigma_X v_{\text{rel}})_0 + (\sigma_{\phi\phi} v_{\text{rel}})_0$ . The thermally averaged total annihilation cross section after including the Sommerfeld enhancement has the form

$$\langle \sigma_{\text{tot}} v_{\text{rel}} \rangle(x) = \langle S_0(v_{\text{rel}}) \rangle(x) (\sigma_X v_{\text{rel}})_0 + \langle S(v_{\text{rel}}) \rangle(x) (\sigma_{\phi\phi} v_{\text{rel}})_0, \quad (15)$$



where  $S(v_{\text{rel}}) = S_{0(1)}(v_{\text{rel}})$ , if the annihilation  $\bar{\chi}\chi \rightarrow \phi\phi$  proceeds through  $s(p)$ -wave. In order to achieve the maximal Sommerfeld enhancement factor, we have assumed that  $\bar{\chi}\chi \rightarrow X$  is an  $s$ -wave process, and both  $X$  and the decay products of  $\phi$  are dominated by SM charged leptons. The boost factor of the DM annihilation is defined as

$$B \equiv \left(\frac{\rho}{\rho_0}\right)^2 \frac{\langle\sigma_{\text{tot}}v_{\text{rel}}\rangle(x_{\text{now}})}{\langle\sigma v_{\text{rel}}\rangle_F}, \quad (16)$$

where  $\rho$  is the DM local energy density, and  $\rho_0 \approx 0.4 \text{ GeVcm}^{-3}$  is the DM energy density estimated from smooth DM density profiles. In this work, we do not consider the boost factor from the local clumps of substructure, namely,  $\rho \approx \rho_0$  is assumed. We parametrize the unknown cross section  $\langle S_0(v_{\text{rel}})\rangle(x)(\sigma_X v_{\text{rel}})_0$  at freeze out as  $\langle S_0(v_{\text{rel}})\rangle(x_f)(\sigma_X v_{\text{rel}})_0 \equiv \eta\langle\sigma v_{\text{rel}}\rangle_F$ . The boost factor can be rewritten as

$$B \approx \eta S_{\text{eff}} + \frac{\langle S(v_{\text{rel}})(\sigma_{\phi\phi} v_{\text{rel}})_0\rangle(x_{\text{now}})}{\langle\sigma v_{\text{rel}}\rangle_F}, \quad (17)$$

where  $S_{\text{eff}} \equiv \langle S_0(v_{\text{rel}})\rangle(x_{\text{now}})/\langle S_0(v_{\text{rel}})\rangle(x_f)$  is the present-day  $s$ -wave Sommerfeld enhancement relative to that at freeze out. The Sommerfeld enhancement factors  $\langle S_{0,1}\rangle$  and the cross section  $(\sigma_{\phi\phi} v_{\text{rel}})_0$  depend on the parameters  $\alpha$  and  $\eta$ . The requirement of reproducing the correct thermal relic density constrains the sizes of  $\alpha$  and  $\eta$ , which will in turn limit the maximally allowed boost factor  $B$ .

### 3.1 Vector boson force-carrier

If the force carrier is a vector gauge boson, the induced potential from the multiple exchange of  $\phi$  between the DM particles is of Yukawa type in Eq. (7). For a vector force carrier, the DM particles can annihilate into  $\phi\phi$  through  $t$ -channel diagram as shown in the right panel of Fig. 1, which is an  $s$ -wave process. The corresponding cross section reads

$$(\sigma_{\phi\phi} v_{\text{rel}})_0^{\text{vec}} = \frac{\pi\alpha^2}{m_\chi^2}. \quad (18)$$

According to Eq. (15), for a given value of  $\eta$ , from calculating the DM thermal relic density and matching it to the observed value in Eq. (14), one can obtain the allowed values of the coupling  $\alpha$  as a function of DM particle mass. The results are shown in the left panel of Fig. 2. At  $m_\chi \approx 460 \text{ GeV}$ , for  $\eta = 0$ , the allowed coupling  $\alpha$  is 0.01. For larger  $\eta$ , the allowed  $\alpha$  in general becomes smaller, as the cross section  $(\sigma_{\phi\phi} v_{\text{rel}})_0$  has to be smaller. Making use of the allowed values of  $\alpha$ , the allowed values of the boost factor  $B$  are calculated, and shown in the  $(m_\chi, B)$  plane in the right panel of Fig. 2, together with the regions favoured by the AMS-02 and Fermi-LAT experiments at 99% C.L. from a global fit assuming a conventional astrophysical background [14]. The case where



$\eta = 0$  corresponds to the case previously discussed in Ref. [44], and our conclusion is in good agreement with theirs. As can be seen in the figure, in this case, the Sommerfeld enhancement can only marginally explain the data of AMS-02, which requires that the enhancement should be in the resonance region. Since both the  $\bar{\chi}\chi \rightarrow \phi\phi$  and  $\bar{\chi}\chi \rightarrow X$  are  $s$ -wave processes, for nonvanishing  $\eta$ , even stronger upper bounds on the boost factor are obtained for larger values of  $\eta$ .

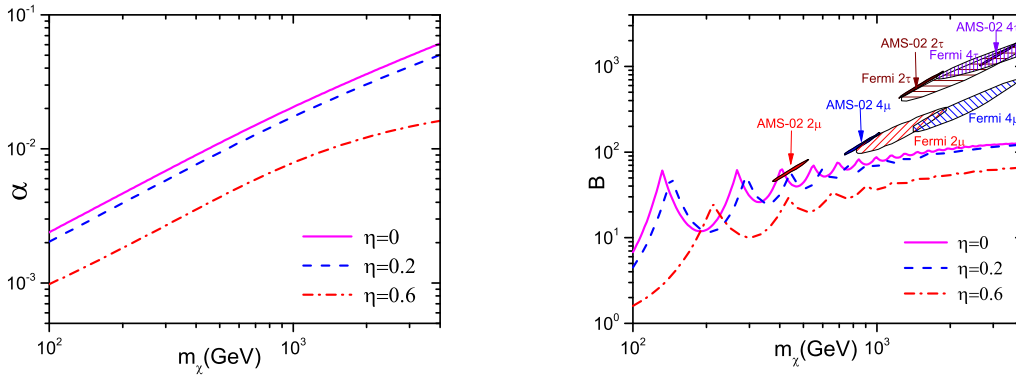


FIG. 2: (Left) Values of  $\alpha$  constrained by the DM relic density as a function of DM particle mass  $m_\chi$  for  $\eta = 0, 0.2$  and  $0.6$ , respectively, in the case where  $\phi$  is a vector boson. (Right) Allowed values of boost factor  $B$  as a function of  $m_\chi$ . The favoured regions at 99% C.L. from a global fit to the data of AMS-02 and Fermi-LAT are also shown [14]. The mass of the vector force-carrier is fixed at  $m_\phi = 0.25$  GeV.

### 3.2 Scalar force-carrier

In the case where the force carrier is a scalar particle, the  $t$ -channel annihilation  $\bar{\chi}\chi \rightarrow \phi\phi$  is a  $p$ -wave process which has a velocity-dependent cross section

$$(\sigma_{\phi\phi}v_{\text{rel}})_0^{\text{sca}} = \frac{3\pi\alpha^2}{8m_\chi^2}v_{\text{rel}}^2. \quad (19)$$

In principle, there could exist non-negligible cubic self-interactions between the force-carriers of the form  $-\mu\phi^3/3!$ , which leads to an additional  $s$ -channel two-body annihilation. The total annihilation cross section is modified as  $(\sigma_{\phi\phi}v_{\text{rel}})_0^{\text{sca}} = (3\pi\alpha^2/(8m_\chi^2))(1 - 5\xi/18 + \xi^2/48)v_{\text{rel}}^2$  with  $\xi = \mu/(2m_\chi\sqrt{\alpha\pi})$  [56]. In this work, for simplicity, we only consider the case where  $\xi \ll 1$ , namely, the  $t$ -channel diagram dominates. Compared with Eq. (18), the cross section of DM annihilating into the scalar force-carriers in Eq. (19) is suppressed by both the prefactor  $3/8$  and the small relative velocity  $v_{\text{rel}}^2 \sim 0.1$  at freeze

out. The corresponding constraint on  $\alpha$  from the DM thermal relic density is expected to be weaker. In the left panel of Fig. 3, we show the allowed value of  $\alpha$  as a function of DM particle mass from the constraint of DM thermal relic density. In the numerical calculations, the Sommerfeld enhancement for the  $p$ -wave process in Eq. (19) is also included. For  $\eta = 0$ , at  $m_\chi = 500$  GeV, the allowed value of coupling  $\alpha$  is  $\sim 0.02$  which is about a factor of two larger than that in the case with a vector force-carrier. In the right panel of Fig. 3, the allowed boost factors are shown for three different choices of  $\eta = 0, 0.46$  and  $0.6$ , respectively. Contrary to the vector force-carrier case, for  $\eta = 0$ , the allowed boost factor is very small, which is due to the fact that in this case the  $p$ -wave annihilation  $\bar{\chi}\chi \rightarrow \phi\phi$  for scalar force-carriers is velocity-suppressed after including the Sommerfeld enhancement. For nonzero  $\eta$ , the allowed boost factor becomes larger. However, the boost factor does not increase monotonically with increasing  $\eta$ . We find that the maximally allowed boost factor at  $m_\chi \approx 460$  GeV corresponds to  $\eta \approx 0.46$ , which can be consistent with that favoured by the AMS-02 data for DM annihilating into  $2\mu$  final states, but is not large enough to account for other final states such as  $2\tau$  and  $4\mu$ . In Fig. 4, we show how the values of  $\alpha$  and the boost factor  $B$  depend on the value of  $\eta$  for a fixed  $m_\chi \approx 460$  GeV for both vector and scalar force-carrier cases. As seen in the figure, for  $\eta \approx 0.46$ , the Sommerfeld enhancement is close to a resonance, which leads to a relatively large boost factor shown in Fig. 3. The effect of resonance is less significant for vector force-carrier case.

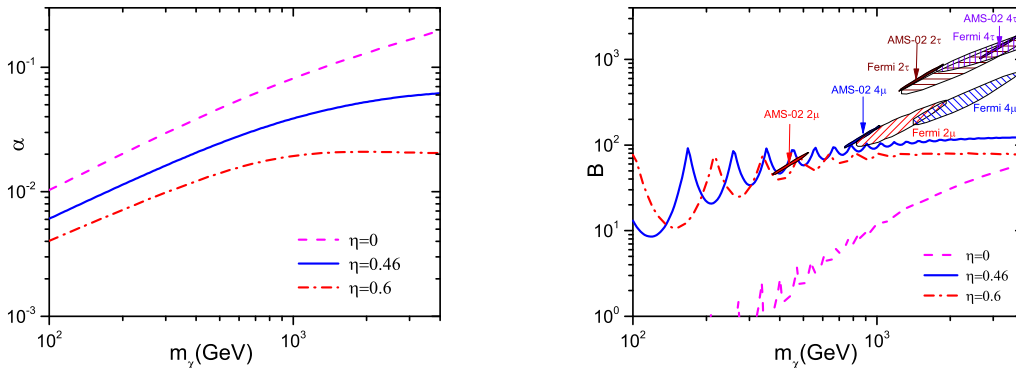


FIG. 3: The same as Fig. 2, but for the case where the force-carrier  $\phi$  is a scalar particle.

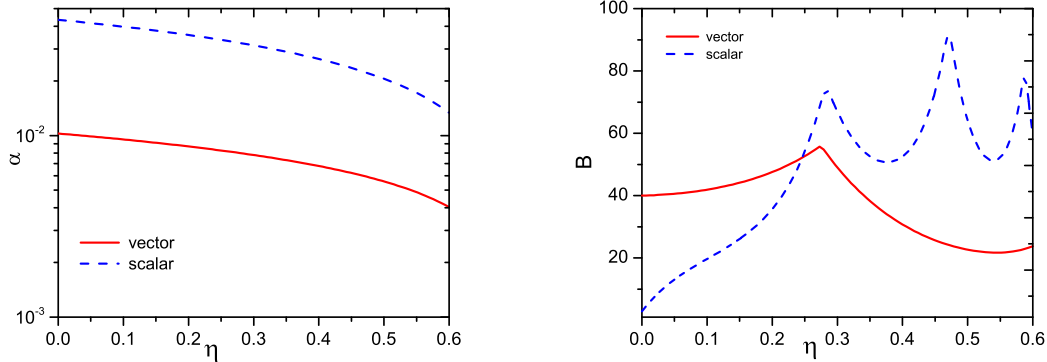


FIG. 4: Comparison between the cases with vector and scalar force-carriers on the allowed values of  $\alpha$  (left) and boost factor  $B$  (right) as a function of  $\eta$ . The masses of the DM particle and the force-carrier are fixed at  $m_\chi = 460$  GeV and  $m_\phi = 0.25$  GeV, respectively.

### 3.3 Pseudoscalar force-carrier

The interaction between a pseudoscalar force-carrier particle  $\phi$  and a fermionic DM particle  $\chi$  is of the form  $i\bar{\chi}\gamma^5\chi\phi$ , which results in a spin-dependent potential

$$V(r) = -\frac{\alpha}{4m_\chi^2 r^3} e^{-m_\phi r} [3(\hat{\mathbf{r}} \cdot \hat{\mathbf{s}}_1)(\hat{\mathbf{r}} \cdot \hat{\mathbf{s}}_2) - \hat{\mathbf{s}}_1 \cdot \hat{\mathbf{s}}_2], \quad (20)$$

where  $\hat{\mathbf{r}}$  is the unit vector along the direction of the relative distance  $\mathbf{r}$  of the two annihilating DM particles, and  $\hat{\mathbf{s}}_{1,2}$  are the unit vectors of the spin orientation of the DM particles. This type of potential is known as the tensor-force potential in nuclear physics and is similar to the potential induced by interaction of two electric dipoles. The Sommerfeld enhancement from this type of potential was discussed previously in Ref. [46] without considering the constraints from DM thermal relic density.

The spin-dependent part of the potential can be rewritten as:  $3(\hat{\mathbf{r}} \cdot \hat{\mathbf{s}}_1)(\hat{\mathbf{r}} \cdot \hat{\mathbf{s}}_2) - \hat{\mathbf{s}}_1 \cdot \hat{\mathbf{s}}_2 = \pm(3\cos^2\theta - 1)$  for  $\hat{\mathbf{s}}_1 = \pm\hat{\mathbf{s}}_2$ , where  $\theta$  is the angle between vectors  $\hat{\mathbf{r}}$  and  $\hat{\mathbf{s}}_1$ . The induced long-range force can be either attractive or repulsive, depending on the relative direction and the spin orientation of the annihilating DM particles. In the case where the force is attractive (repulsive), Sommerfeld enhancements (suppressions) of DM annihilation can occur. Although for unpolarized initial states of DM particles, the chances are equal for the forces to be attractive or repulsive, the net effect of the Sommerfeld enhancements and suppressions on the DM annihilation rate can be nonzero, as the enhancement of the annihilation rates can be dominant. In this work, we consider the case where the spins of two annihilating DM particles are parallel, i.e.,  $\hat{\mathbf{s}}_1 = \hat{\mathbf{s}}_2$ , and calculate the corresponding

Sommerfeld enhancement factors. The Sommerfeld suppression in the antiparallel case is taken into account by adding an overall suppression factor  $1/2$  to the boost factor  $B$ , which corresponds to the maximal suppression effect.

The potential matrix in the angular momentum space can be written in terms of the Wigner  $3 - j$  symbol as

$$V_{\ell\ell'}(r) = -\frac{\alpha e^{-m_\phi r}}{m_\chi^2 r^3} \sqrt{(2\ell+1)(2\ell'+1)} \begin{pmatrix} \ell & 2 & \ell' \\ 0 & 0 & 0 \end{pmatrix}^2. \quad (21)$$

The off-diagonal elements of  $V_{\ell\ell'}$  are nonvanishing for any  $\ell$  and  $\ell'$  satisfying  $|\ell' - \ell| = 2$ . Thus the Schrödinger equations for different partial waves are all coupled together. We solve the coupled Schrödinger equations using the Born-Oppenheimer adiabatic approximation. In this approach, a spatial-dependent rotation matrix  $U_{i\ell}(r)$  is introduced to locally diagonalize the sum of the potential and the centrifugal term in the Schrödinger equation at the position  $r$

$$H(r)_{ij} = U_{i\ell}(r) \left[ m_\chi V_{\ell\ell'}(r) + \frac{\ell(\ell+1)}{r^2} \delta_{\ell\ell'} \right] U_{\ell'j}^T(r), \quad (22)$$

where  $H(r)$  is a diagonal matrix. In this basis, the only off-diagonal terms in the Schrödinger equation are proportional to  $dU/dr$  or  $d^2U/dr^2$ . For slowly varying potential (in comparison with the Compton wave length of the particle falling into the center) the terms proportional to  $dU/dr$  and  $d^2U/dr^2$  are relatively small and can be neglected as a first order approximation. Under this adiabatic approximation, the Schrödinger equations for the rotated wave function  $\phi_i(r) = U_{i\ell}(r)\chi_\ell(r)$  are decoupled, and have the simple form [57]

$$\frac{d^2}{dr^2}\phi_i - H(r)\phi_i + k^2\phi_i \simeq 0, \quad (23)$$

which can be solved easily with the rotated boundary conditions. The solutions and the Sommerfeld enhancement factors for each partial wave are obtained by performing an inverse rotation back into the original basis with definite angular momentum. Note that in the limit  $r \rightarrow \infty$  the centrifugal term  $\ell(\ell+1)/r^2$  dominates over  $V_{\ell\ell'}$ . The rotation matrix in this limit is a unit matrix. In numerical calculations, we consider the angular momentum up to  $\ell = 8$ , thus  $V_{\ell\ell'}$  is a matrix of dimension-nine. We find good stability in the solutions of the wave functions with lowest indices  $\phi_{1,2}$ .

It is known in quantum mechanics that for an attractive potential scaling with distance as  $r^{-s}$  with  $s \geq 2$ , the wave function is not well-defined (divergent) at the origin. A procedure of regularization of this type of potential has to be introduced, which represents the nonfactorizable contributions from the short-distance (for a review, see Ref [58]). In this work, we adopt a commonly used regularization scheme

$$V(r) \rightarrow V(r + r_0), \quad (24)$$

where  $r_0$  is a cut-off parameter. In the generic case, the pseudoscalar induced potential can be regularized as  $r^{-3} \rightarrow r^{-\beta}(r + r_0)^{\beta-3}$  with  $\beta < 2$ . The regularization scheme in Eq. (24) corresponds to the case where  $\beta = 0$ . We have also performed calculations for the case of  $\beta = 1$  and find no significant changes in the conclusions.

In Fig. 5, we show how the thermally averaged Sommerfeld enhancement factor  $\langle S \rangle$  depends on the coupling strength  $\alpha$  and cut-off parameter  $r_0$  for both  $s$ - and  $p$ -wave annihilation at the temperature  $x = x_{\text{now}}$ . Similar to the case with Yukawa potential, in some regions of parameter space, resonant Sommerfeld enhancement occurs, which corresponds to the formation of zero-energy bound states. We find that at the resonance points, the parameters  $\alpha$ ,  $r_0$ , and  $m_\chi$  satisfy the following approximate relation

$$\alpha \approx \frac{r_0}{R} n m_\chi, \quad (25)$$

where  $n = 1, 2, 3, \dots$ , and  $R \approx 0.0347$  ( $0.0227$ ) for  $s(p)$ -wave annihilation. As expected, the enhancement factors become larger with increasing  $\alpha$  and decreasing  $r_0$ . As shown

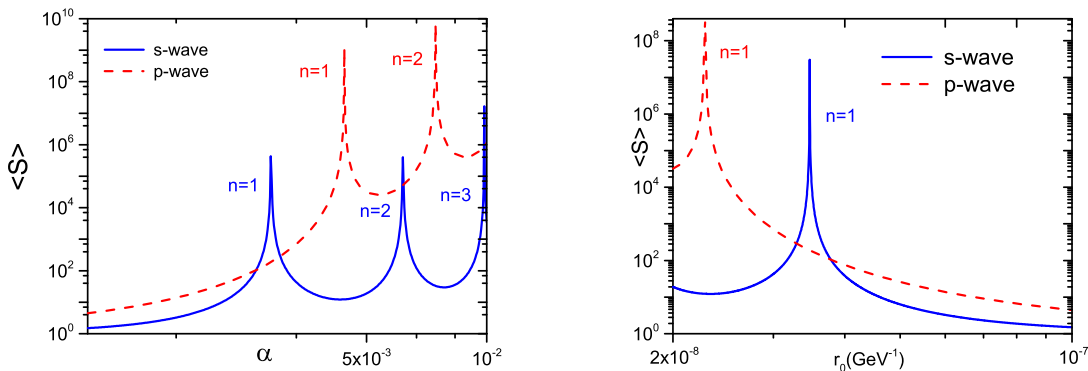


FIG. 5:  $s$ -wave and  $p$ -wave thermally averaged Sommerfeld enhancement factors  $\langle S \rangle$  as a function of  $\alpha$  (left) and the cut-off scale  $r_0$  (right) for  $x = x_{\text{now}}$ . In the left panel,  $r_0$  is fixed at  $1.0 \times 10^{-7} \text{ GeV}^{-1}$ , while in the right panel  $\alpha$  is fixed at 0.001. The masses of the DM particle and the force-carrier are fixed at  $m_\chi = 1000 \text{ GeV}$  and  $m_\phi = 0.25 \text{ GeV}$ , respectively.

in Eq. (16), the boost factor depends only on the size of the Sommerfeld enhancement at the present day relative to that at the time of freeze out. For the regularized singular potentials, only at the resonance points, the Sommerfeld enhancement factor depends significantly on the temperature. In Fig. 6, we show the thermally averaged Sommerfeld enhancement factor of pseudoscalar induced potential for  $s$ - and  $p$ -wave cases. The parameters are chosen to be  $\alpha = 2.88 \times 10^{-3}$ ,  $r_0 = 1.0 \times 10^{-7} \text{ GeV}^{-1}$ , and  $m_\chi = 1 \text{ TeV}$ ,

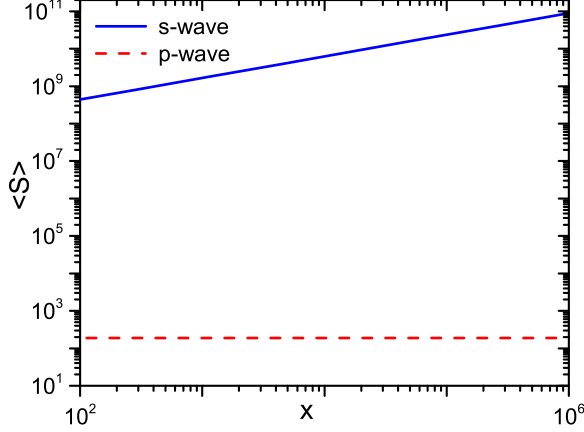


FIG. 6: Temperature dependence of the thermally averaged Sommerfeld enhancement factor in the  $s$ -wave resonance region, corresponding to the resonance point with  $r_0 = 1.0 \times 10^{-7} \text{ GeV}^{-1}$ ,  $\alpha = 2.880 \times 10^{-3}$  and  $n = 1$  as shown in Fig. 5. Other parameters are  $m_\chi = 1000 \text{ GeV}$ , and  $m_\phi = 0.25 \text{ GeV}$ . The  $p$ -wave Sommerfeld enhancement factor is also shown, which shows no visible temperature dependence as it is off-resonance for the chosen parameters.

which corresponds to the  $s$ -wave resonance point with  $n = 1$ . From the figure, one sees that the thermally averaged Sommerfeld enhancement factor at  $x \approx x_{\text{now}}$  can be a few hundred times larger than that at freeze out  $x \approx x_f$ . For the same parameter set, the  $p$ -wave annihilation is not at the resonance point, thus there is no relative enhancement towards low temperatures. This feature is similar to the case with a spherical well potential  $V_{\text{well}}(r) = -V_0\theta(r - r_0)$  with  $\theta(x)$  the Heaviside step function. For the spherical well potential, the Sommerfeld enhancement factor for  $s$ -wave annihilation is given by [33]

$$S_0^{\text{well}}(v_{\text{rel}}) = \frac{1}{1 - \frac{V_0}{V_0 + m_\chi v_{\text{rel}}^2/4} \sin^2(r_0 \sqrt{4m_\chi V_0 + m_\chi^2 v_{\text{rel}}^2})}. \quad (26)$$

For a deep well  $V_0 \gg m_\chi v_{\text{rel}}^2/4$ , in the resonant region, i.e.,  $r_0 \sqrt{4m_\chi V_0} \approx n + \pi/2$ , one obtains  $S_0^{\text{well}}(v_{\text{rel}}) \sim 4V_0/(m_\chi v_{\text{rel}}^2)$ . But when it is off-resonance,  $S_0^{\text{well}}(v_{\text{rel}}) \approx 1$ .

We proceed to discuss the constraints on the Sommerfeld enhancement from DM thermal relic density. For the pseudoscalar force carrier  $\phi$ , the cross section for the  $t$ -channel DM annihilation process  $\bar{\chi}\chi \rightarrow 2\phi$  is given by

$$(\sigma_{2\phi} v_{\text{rel}})_0^{\text{ps}} = \frac{\pi\alpha^2}{24m_\chi^2} v_{\text{rel}}^2. \quad (27)$$

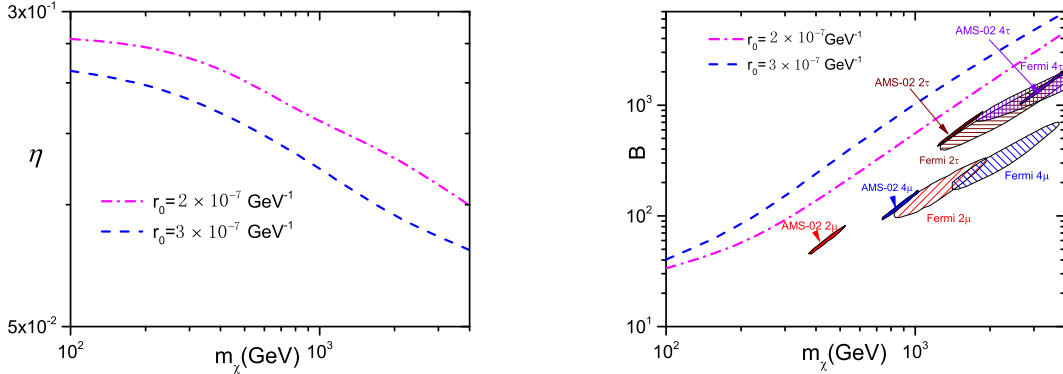


FIG. 7: (Left) Values of  $\eta$  constrained by the DM thermal relic density as a function of DM particle mass with two different cut-offs  $r_0 = 2.0 \times 10^{-7} \text{ GeV}^{-1}$  and  $3.0 \times 10^{-7} \text{ GeV}^{-1}$ . (Right) The allowed boost factors as a function of DM particle mass. The mass of pseudoscalar force-carrier is fixed at  $m_\phi = 0.25 \text{ GeV}$ .

Compared with the cross section of the scalar force-carrier case in Eq. (19), it is smaller by a factor of nine, which results in a weaker constraint from thermal relic density. Since at the resonance points the coupling strength  $\alpha$  is related to other parameters such as  $r_0$  and  $m_\chi$  through Eq. (25), we show instead in the left panel of Fig. 7 the constraints on the parameter  $\eta$ , for two different cut-offs  $r_0 = 2.0 \times 10^{-7} \text{ GeV}^{-1}$  and  $3.0 \times 10^{-7} \text{ GeV}^{-1}$ , respectively. The decrease of  $\eta$  at larger  $m_\chi$ , is due to the increase of  $\langle S \rangle(x_f)$ , as  $\alpha$  is related to  $m_\chi$  through Eq. (25). For larger  $r_0$ , the value of  $\alpha$  is larger, thus the required  $\eta$  becomes smaller. The allowed boost factors at the present day are shown in the right panel of Fig. 7. One sees that in the case with pseudoscalar force carrier, the allowed Sommerfeld enhancement factors can be large enough to account for the excesses reported by AMS-02 and Fermi-LAT for a variety of final states such as  $2\mu$ ,  $2\tau$ ,  $4\mu$  and  $4\tau$ , etc..

## 4 Conclusions

Although the Sommerfeld enhancement has been considered as a mechanism for naturally increasing the DM annihilation cross section at low relative velocities, which is crucial to explain the current data of PAMELA, Fermi-LAT and AMS-02, stringent constraint can arise from the DM thermal relic density, partially due to the annihilation of DM particles into the force-carriers introduced by this mechanism. We have shown that the effect of the Sommerfeld enhancement and the constraint from thermal relic density depend on



the nature of the force-carrier particle. For the force-carrier being a vector boson, the induced long-range potential is of Yukawa type, and the process of  $\bar{\chi}\chi \rightarrow \phi\phi$  is an  $s$ -wave process. If  $\phi$  is a scalar, the same process becomes a velocity-suppressed  $p$ -wave process, which resulting in a weaker constraint. If  $\phi$  is a pseudoscalar, the induced long-range potential is a tensor force, and  $\bar{\chi}\chi \rightarrow \phi\phi$  is again a  $p$ -wave process. We have explored and compared the Sommerfeld enhancements with these three type of force-carriers under the constraint from DM thermal relic density. The results show that for vector boson force-carrier the Sommerfeld enhancement can only marginally account for the AMS-02 data, for scalar force-carrier the allowed Sommerfeld enhancement factor can be larger roughly by a factor of two, while in the case of pseudoscalar force carrier, much larger enhancement can be obtained in the resonance region. The Sommerfeld enhancement may still be a viable mechanism to account for the current cosmic-ray lepton anomalies.

## Acknowledgments

This work is supported in part by the National Basic Research Program of China (973 Program) under Grants No. 2010CB833000; the National Nature Science Foundation of China (NSFC) under Grants No. 10975170, No. 10821504 and No. 10905084; and the Project of Knowledge Innovation Program (PKIP) of the Chinese Academy of Science.

## References

- [1] **Planck Collaboration**, P. Ade *et. al.*, *Planck 2013 results. I. Overview of products and scientific results*, [arXiv:1303.5062](#).
- [2] **Planck Collaboration**, P. Ade *et. al.*, *Planck 2013 results. XVI. Cosmological parameters*, [arXiv:1303.5076](#).
- [3] **PAMELA Collaboration**, O. Adriani *et. al.*, *An anomalous positron abundance in cosmic rays with energies 1.5-100 GeV*, *Nature* **458** (2009) 607–609, [[arXiv:0810.4995](#)].
- [4] O. Adriani, G. Barbarino, G. Bazilevskaya, R. Bellotti, M. Boezio, *et. al.*, *A statistical procedure for the identification of positrons in the PAMELA experiment*, *Astropart.Phys.* **34** (2010) 1–11, [[arXiv:1001.3522](#)].
- [5] **Fermi LAT Collaboration**, M. Ackermann *et. al.*, *Measurement of separate cosmic-ray electron and positron spectra with the Fermi Large Area Telescope*, *Phys.Rev.Lett.* **108** (2012) 011103, [[arXiv:1109.0521](#)].

- [6] J. Chang *et. al.*, *An excess of cosmic ray electrons at energies of 300-800 GeV*, *Nature* **456** (2008) 362–365.
- [7] **The Fermi LAT** Collaboration, A. A. Abdo *et. al.*, *Measurement of the Cosmic Ray  $e^+$  plus  $e^-$  spectrum from 20 GeV to 1 TeV with the Fermi Large Area Telescope*, *Phys. Rev. Lett.* **102** (2009) 181101, [[arXiv:0905.0025](#)].
- [8] **Fermi LAT Collaboration** , M. Ackermann *et. al.*, *Fermi LAT observations of cosmic-ray electrons from 7 GeV to 1 TeV*, *Phys.Rev.* **D82** (2010) 092004, [[arXiv:1008.3999](#)].
- [9] **AMS Collaboration** , e. Aguilar, M., *First result from the alpha magnetic spectrometer on the international space station: Precision measurement of the positron fraction in primary cosmic rays of 0.5~350 gev*, *Phys. Rev. Lett.* **110** (Apr, 2013) 141102.
- [10] J. Kopp, *Constraints on dark matter annihilation from AMS-02 results*, [arXiv:1304.1184](#).
- [11] A. De Simone, A. Riotto, and W. Xue, *Interpretation of AMS-02 Results: Correlations among Dark Matter Signals*, [arXiv:1304.1336](#).
- [12] Q. Yuan, X.-J. Bi, G.-M. Chen, Y.-Q. Guo, S.-J. Lin, *et. al.*, *Implications of the AMS-02 positron fraction in cosmic rays*, [arXiv:1304.1482](#).
- [13] I. Cholis and D. Hooper, *Dark Matter and Pulsar Origins of the Rising Cosmic Ray Positron Fraction in Light of New Data From AMS*, [arXiv:1304.1840](#).
- [14] H.-B. Jin, Y.-L. Wu, and Y.-F. Zhou, *Implications of the first AMS-02 measurement for dark matter annihilation and decay*, [arXiv:1304.1997](#).
- [15] Q. Yuan and X.-J. Bi, *Reconcile the AMS-02 positron fraction and Fermi-LAT/HESS total  $e^\pm$  spectra by the primary electron spectrum hardening*, [arXiv:1304.2687](#).
- [16] Y. Kajiyama, H. Okada, and T. Toma, *New Interpretation of the Recent Result of AMS-02 and Multi-component Decaying Dark Matters with non-Abelian Discrete Flavor Symmetry*, [arXiv:1304.2680](#).
- [17] L. Feng and Z. Kang, *Decaying Asymmetric Dark Matter Relaxes the AMS-Fermi Tension*, [arXiv:1304.7492](#).
- [18] A. Sommerfeld, *Annalen der Physik*, 403, 257 (1931).

- [19] J. Hisano, S. Matsumoto, and M. M. Nojiri, *Unitarity and higher-order corrections in neutralino dark matter annihilation into two photons*, *Phys. Rev.* **D67** (2003) 075014, [[hep-ph/0212022](#)].
- [20] J. Hisano, S. Matsumoto, and M. M. Nojiri, *Explosive dark matter annihilation*, *Phys. Rev. Lett.* **92** (2004) 031303, [[hep-ph/0307216](#)].
- [21] M. Cirelli, A. Strumia, and M. Tamburini, *Cosmology and Astrophysics of Minimal Dark Matter*, *Nucl. Phys.* **B787** (2007) 152–175, [[arXiv:0706.4071](#)].
- [22] N. Arkani-Hamed, D. P. Finkbeiner, T. R. Slatyer, and N. Weiner, *A Theory of Dark Matter*, *Phys. Rev.* **D79** (2009) 015014, [[arXiv:0810.0713](#)].
- [23] M. Pospelov and A. Ritz, *Astrophysical Signatures of Secluded Dark Matter*, *Phys. Lett.* **B671** (2009) 391–397, [[arXiv:0810.1502](#)].
- [24] J. D. March-Russell and S. M. West, *WIMPonium and Boost Factors for Indirect Dark Matter Detection*, *Phys. Lett.* **B676** (2009) 133–139, [[arXiv:0812.0559](#)].
- [25] R. Iengo, *Sommerfeld enhancement: general results from field theory diagrams*, *JHEP* **05** (2009) 024, [[arXiv:0902.0688](#)].
- [26] S. Cassel, *Sommerfeld factor for arbitrary partial wave processes*, *J. Phys.* **G37** (2010) 105009, [[arXiv:0903.5307](#)].
- [27] D. Feldman, Z. Liu, and P. Nath, *PAMELA Positron Excess as a Signal from the Hidden Sector*, *Phys. Rev.* **D79** (2009) 063509, [[arXiv:0810.5762](#)].
- [28] M. Ibe, H. Murayama, and T. T. Yanagida, *Breit-Wigner Enhancement of Dark Matter Annihilation*, *Phys. Rev.* **D79** (2009) 095009, [[arXiv:0812.0072](#)].
- [29] W.-L. Guo and Y.-L. Wu, *Enhancement of Dark Matter Annihilation via Breit-Wigner Resonance*, *Phys. Rev.* **D79** (2009) 055012, [[arXiv:0901.1450](#)].
- [30] Z.-P. Liu, Y.-L. Wu, and Y.-F. Zhou, *Enhancement of dark matter relic density from the late time dark matter conversions*, *Eur.Phys.J.* **C71** (2011) 1749, [[arXiv:1101.4148](#)].
- [31] Z.-P. Liu, Y.-L. Wu, and Y.-F. Zhou, *Dark Matter Conversion as a Source of Boost Factor for Explaining the Cosmic Ray Positron and Electron Excesses*, *J.Phys.Conf.Ser.* **384** (2012) 012024, [[arXiv:1112.4030](#)].

- [32] J. Zavala, M. Vogelsberger, and S. D. M. White, *Relic density and CMB constraints on dark matter annihilation with Sommerfeld enhancement*, *Phys. Rev. D* **D81** (2010) 083502, [arXiv:0910.5221].
- [33] S. Hannestad and T. Tram, *Sommerfeld Enhancement of DM Annihilation: Resonance Structure, Freeze-Out and CMB Spectral Bound*, *JCAP* **1101** (2011) 016, [arXiv:1008.1511].
- [34] J. Hisano *et. al.*, *Cosmological constraints on dark matter models with velocity-dependent annihilation cross section*, *Phys. Rev. D* **D83** (2011) 123511, [arXiv:1102.4658].
- [35] M. Kamionkowski and S. Profumo, *Early Annihilation and Diffuse Backgrounds in Models of Weakly Interacting Massive Particles in Which the Cross Section for Pair Annihilation Is Enhanced by  $1/v$* , *Phys. Rev. Lett.* **101** (2008) 261301, [arXiv:0810.3233].
- [36] J. Bovy, *Substructure Boosts to Dark Matter Annihilation from Sommerfeld Enhancement*, *Phys. Rev. D* **D79** (2009) 083539, [arXiv:0903.0413].
- [37] M. R. Buckley and P. J. Fox, *Dark Matter Self-Interactions and Light Force Carriers*, *Phys. Rev. D* **D81** (2010) 083522, [arXiv:0911.3898].
- [38] J. L. Feng, M. Kaplinghat, and H.-B. Yu, *Halo Shape and Relic Density Exclusions of Sommerfeld-Enhanced Dark Matter Explanations of Cosmic Ray Excesses*, *Phys. Rev. Lett.* **104** (2010) 151301, [arXiv:0911.0422].
- [39] I. Cholis and L. Goodenough, *Consequences of a Dark Disk for the Fermi and PAMELA Signals in Theories with a Sommerfeld Enhancement*, *JCAP* **1009** (2010) 010, [arXiv:1006.2089].
- [40] M. Lattanzi and J. I. Silk, *Can the WIMP annihilation boost factor be boosted by the Sommerfeld enhancement?*, *Phys. Rev. D* **D79** (2009) 083523, [arXiv:0812.0360].
- [41] B. Robertson and A. Zentner, *Dark Matter Annihilation Rates with Velocity-Dependent Annihilation Cross Sections*, *Phys. Rev. D* **D79** (2009) 083525, [arXiv:0902.0362].
- [42] M. Cirelli and J. M. Cline, *Can multistate dark matter annihilation explain the high-energy cosmic ray lepton anomalies?*, *Phys. Rev. D* **D82** (2010) 023503, [arXiv:1005.1779].

- [43] K. N. Abazajian and J. P. Harding, *Constraints on WIMP and Sommerfeld-Enhanced Dark Matter Annihilation from HESS Observations of the Galactic Center*, [arXiv:1110.6151](#).
- [44] J. L. Feng, M. Kaplinghat, and H.-B. Yu, *Sommerfeld Enhancements for Thermal Relic Dark Matter*, *Phys. Rev.* **D82** (2010) 083525, [[arXiv:1005.4678](#)].
- [45] J. March-Russell, S. M. West, D. Cumberbatch, and D. Hooper, *Heavy Dark Matter Through the Higgs Portal*, *JHEP* **0807** (2008) 058, [[arXiv:0801.3440](#)].
- [46] P. F. Bedaque, M. I. Buchoff, and R. K. Mishra, *Sommerfeld enhancement from Goldstone pseudo-scalar exchange*, *JHEP* **0911** (2009) 046, [[arXiv:0907.0235](#)].
- [47] J. Hisano, S. Matsumoto, M. M. Nojiri, and O. Saito, *Non-perturbative effect on dark matter annihilation and gamma ray signature from galactic center*, *Phys.Rev.* **D71** (2005) 063528, [[hep-ph/0412403](#)].
- [48] R. Iengo, *Sommerfeld enhancement for a Yukawa potential*, [arXiv:0903.0317](#).
- [49] T. R. Slatyer, *The Sommerfeld enhancement for dark matter with an excited state*, *JCAP* **1002** (2010) 028, [[arXiv:0910.5713](#)].
- [50] A. Hryczuk, R. Iengo, and P. Ullio, *Relic densities including Sommerfeld enhancements in the MSSM*, *JHEP* **03** (2011) 069, [[arXiv:1010.2172](#)].
- [51] J. B. Dent, S. Dutta, and R. J. Scherrer, *Thermal Relic Abundances of Particles with Velocity- Dependent Interactions*, *Phys. Lett.* **B687** (2010) 275–279, [[arXiv:0909.4128](#)].
- [52] D. P. Finkbeiner, L. Goodenough, T. R. Slatyer, M. Vogelsberger, and N. Weiner, *Consistent Scenarios for Cosmic-Ray Excesses from Sommerfeld-Enhanced Dark Matter Annihilation*, *JCAP* **1105** (2011) 002, [[arXiv:1011.3082](#)].
- [53] A. Hryczuk and R. Iengo, *The one-loop and Sommerfeld electroweak corrections to the Wino dark matter annihilation*, *JHEP* **1201** (2012) 163, [[arXiv:1111.2916](#)].
- [54] K. L. McDonald, *Sommerfeld Enhancement from Multiple Mediators*, *JHEP* **1207** (2012) 145, [[arXiv:1203.6341](#)].
- [55] S. Tulin, H.-B. Yu, and K. M. Zurek, *Beyond Collisionless Dark Matter: Particle Physics Dynamics for Dark Matter Halo Structure*, [arXiv:1302.3898](#).
- [56] J. Chen and Y.-F. Zhou, *The 130 GeV gamma-ray line and Sommerfeld enhancements*, *JCAP* **1304** (2013) 017, [[arXiv:1301.5778](#)].

- [57] V. Roudnev and M. Cavagnero, *Resonance phenomena in ultracold dipole-dipole scattering*, *Journal of Physics B Atomic Molecular Physics* **42** (Feb., 2009) 044017–+, [arXiv:0809.2566].
- [58] W. Frank, D. Land, and R. Spector, *Singular potentials*, *Rev.Mod.Phys.* **43** (1971) 36–98.